

Electron Depletion Due to Bias of a T-Shaped Field-Effect Transistor

G. A. Georgakis and Qian Niu

Department of Physics, University of Texas at Austin, Austin, Texas 78712

(December 23, 2018)

Abstract

A T-shaped field-effect transistor, made out of a pair of two-dimensional electron gases, is modeled and studied. A simple numerical model is developed to study the electron distribution vs. applied gate voltage for different gate lengths. The model is then improved to account for depletion and the width of the two-dimensional electron gases. The results are then compared to the experimental ones and to some approximate analytical calculations and are found to be in good agreement with them.

02.60.cb, 02.60.Nm, 79.60.Jv, 85.30.De, 85.30.Tv

I. INTRODUCTION

Extensive work has been published on various nano-structure devices that use two-dimensional electron gases (2DEG)^{1,2}. Numerous devices have been built using nanofabrication that involve shaping the 2DEG by applying gate voltages. Some of the techniques use in-plane gating^{3,4}; however, most of them use off-plane gating^{5–7}. Here, we study an off-plane device whose gate is also a 2DEG.

Our work was prompted by a paper by H. L. Stormer et al.⁷ In that paper, a new type of T-shaped field-effect transistor (T-FET) was presented with an ultra short gate length. The transistor is made out of a pair of 2DEGs that are oriented perpendicular to each other. One is used as the source-drain channel, and the other is used as the gate. When the gate voltage exceeds a certain critical value, a depletion region is created in the source-drain channel which cuts off the current flow through it.

The device is made exclusively using molecular beam epitaxy (MBE). The 2DEG of the gate is made by standard modulation doping of a *GaAs* substrate in the following way:

4.3 μm	undoped	$\text{Al}_{0.3}\text{Ga}_{0.7}\text{As}$,
200 \AA	undoped	<i>GaAs</i> quantum well,
150 \AA	undoped	$\text{Al}_{0.3}\text{Ga}_{0.7}\text{As}$ spacer,
$1.5 \times 10^{16} \text{ m}^{-2}$	<i>Si</i> δ doping,	
20 μm	undoped	$\text{Al}_{0.3}\text{Ga}_{0.7}\text{As}$.

Following this, the structure is now cleaved on one edge, and the growth continues in a perpendicular direction. The growth sequence is as follows:

200 \AA	undoped	$\text{Al}_{0.3}\text{Ga}_{0.7}\text{As}$ separator,
150 \AA	undoped	<i>GaAs</i> quantum well,
150 \AA	undoped	$\text{Al}_{0.3}\text{Ga}_{0.7}\text{As}$ spacer,
$2 \times 10^{16} \text{ m}^{-2}$	<i>Si</i> δ doping,	
1700 \AA	undoped	$\text{Al}_{0.3}\text{Ga}_{0.7}\text{As}$,
600 \AA	undoped	<i>GaAs</i> .

This produces a modulation-doped quantum well which is 200 \AA wide for the gate and 150 \AA

wide for the source-drain channel. A cross section of the transistor is shown in Fig. 1.

In Sec. II, we develop a very simple model for the transistor, based on work done by X. Liu and one of us⁸. In this model, we assume that the electron distribution is related to the potential energy by the Thomas-Fermi equation

$$n = (\delta - U)\nu. \quad (1)$$

Here, n is the extra electron distribution due to the applied gate voltage, $\nu = \frac{m^*}{\pi\hbar^2}$ is the two-dimensional density of states, and δ is the change in chemical potential of the two 2DEGs due to the bias. The equation is valid everywhere except inside the insulating barriers and any created depletion regions. It does not give an exact solution to the problem, but it can give a good understanding of the general behavior of this kind of semiconductor device. Furthermore, we initially assume that the two 2DEGs have no width in the direction in which they are confined by the quantum wells, and that the donors that created the gases are in the same position as the 2DEGs. We also assume that no depletion region is created. These assumptions allow us to come up with an analytic solution to the problem using Fourier transforms.

In Sec. III, we allow for a depletion region to be created. The solution using Fourier transforms is no longer feasible, and a numerical solution is used throughout. Special techniques had to be developed for this.

In Sec. IV, we make a more realistic model of the transistor by taking into account the finite width of the gases. The techniques used to solve these are very similar to those used in Sec. III.

In Sec. V, an approximate analytic approach is used for the problem inspired by Ref. 9. The results of the two methods are then compared in the conclusion.

II. THE ONSET OF DEPLETION

As a first approach, we assume that the two 2DEGs have no width and that no depletion region is created. Furthermore, we assume that the donors are in the same position as the

2DEGs. As shown in Fig. 2, we choose the x axis for the gate and the y axis for the source-drain channel. The above assumptions simplify the equations for the potential energy of the gases to

$$U(x, y) = -\frac{e^2}{2\pi\epsilon} \int_a^\infty dx' n_x(x') \log |(x - x')^2 + y^2|^{1/2} - \frac{e^2}{2\pi\epsilon} \int_{-\infty}^\infty dy' n_y(y') \log |x^2 + (y - y')^2|^{1/2}, \quad (2)$$

which on each axis gives

$$U(x) \equiv U(x, 0) = -\frac{e^2}{2\pi\epsilon} \int_a^\infty dx' n_x(x') \log |x - x'| - \frac{e^2}{2\pi\epsilon} \int_{-\infty}^\infty dy' n_y(y') \log |x^2 + y'^2|^{1/2}, \quad (3a)$$

and

$$U(y) \equiv U(0, y) = -\frac{e^2}{2\pi\epsilon} \int_a^\infty dx' n_x(x') \log |x'^2 + y^2|^{1/2} - \frac{e^2}{2\pi\epsilon} \int_{-\infty}^\infty dy' n_y(y') \log |y - y'|. \quad (3b)$$

In addition, for each of the 2DEGs the Thomas-Fermi equations give

$$n(x) = [\delta_x - U(x)]\nu, \quad (4a)$$

and

$$n(y) = [\delta_y - U(y)]\nu \quad (4b)$$

for the x and y axis respectively. Substituting in for the potential energy terms on each axis from Eqs. (3), and rescaling a few of the parameters we get

$$n_x(x) = \delta_x + \frac{2}{\pi} \int_a^\infty dx' n_x(x') \log |x - x'| + \frac{2}{\pi} \int_{-\infty}^\infty dy' n_y(y') \log |x^2 + y'^2|^{1/2}, \quad (5a)$$

and

$$n_y(y) = \delta_y + \frac{2}{\pi} \int_a^\infty dx' n_x(x') \log |x'^2 + y^2|^{1/2} + \frac{2}{\pi} \int_{-\infty}^\infty dy' n_y(y') \log |y - y'|. \quad (5b)$$

The new units used are: length: $a_0 = \frac{4\pi\epsilon\hbar^2}{m^*e^2}$; density: $\frac{m^*eV_g}{\pi\hbar^2} = \frac{eV_g}{E_F} n_0$; voltage: eV_g . These are two integral equations with two unknown functions $n_x(x)$ and $n_y(y)$. In addition to the above equations, the two additional requirements are the neutrality

$$\int_a^\infty dx n_x(x) + \int_{-\infty}^\infty dy n_y(y) = 0, \quad (6)$$

and the fact that

$$\delta_x - \delta_y = 1. \quad (7)$$

The above equation states the fact that the difference in the chemical potentials of the two sides is just the gate voltage.

We can obtain one equation for $n_x(x)$ by using Fourier transforms to eliminate $n_y(y)$.

The resulting integral equation for $n_x(x)$ is

$$n_x(x) = 1 - \frac{2}{\pi} \int_a^\infty dx' n_x(x') \times \left\{ \log \left| \frac{x+x'}{x-x'} \right| + \int_0^\infty dk \frac{e^{-(x+x')k}}{k+2} \right\}. \quad (8)$$

In a very similar way, we can obtain an equation for $n_y(y)$ in terms of $n_x(x)$. By manipulating Eqs. (5), we can express the Fourier transform of $n_y(y)$ in terms of $n_x(x)$ as $\hat{n}_y(k_y) = 2\pi\delta_y \frac{|k_y|\delta(k_y)}{|k_y|+2} - 2 \int_a^\infty dx' n_x(x') \frac{e^{-|k_y|x'}}{|k_y|+2}$ which, after taking the inverse Fourier transform, gives

$$n_y(y) = -\frac{2}{\pi} \int_a^\infty dx' n_x(x') \int_0^\infty dk_y \frac{\cos(k_y y) e^{-k_y x'}}{k_y + 2}. \quad (9)$$

Before trying to solve this equation, we investigate the long range solution. The numerator of the dk integral in Eq. (8) approaches zero quickly as $x \rightarrow \infty$. Assuming that $n_x(x) \sim \frac{\alpha}{x^\beta}$ as $x \rightarrow \infty$, and by setting $t = x/x'$, we must have $1 = \frac{2}{\pi} \frac{\alpha}{x^{\beta-1}} \int_{a/x}^\infty dt' \frac{1}{t^\beta} \log \left| \frac{1+t}{1-t} \right|$. Since $\int_0^\infty dt' \frac{1}{t} \log \left| \frac{1+t}{1-t} \right| = \frac{\pi^2}{2}$, we can infer that $\alpha = \frac{1}{\pi}$ and $\beta = 1$. This gives

$$n_x(x) = \frac{1}{\pi x}, \quad x \rightarrow \infty \quad (10)$$

for the asymptotic form.

For the asymptotic form of $n_y(y)$, we need to manipulate Eq. (9). We first set $k' = k|y|$ which, along with the condition that $y \rightarrow \infty$, enables us to compute the dk integral so that we now have $n_y(y) = -\frac{2}{\pi} \int_a^\infty dx' \frac{1}{x'^2 + y^2}$. The dx' integral can now be computed by using the variable substitution $t = x'/y$. The final result for the asymptotic form of $n_y(y)$ is

$$n_y(y) = \frac{1}{2\pi|y|}, \quad |y| \rightarrow \infty \quad (11)$$

Eq. (8) can be solved either by successive iterations or by using a matrix method, since it is linear. The result is shown in Fig. 3a. $n_y(y)$ can be computed from Eq. (9) since $n_x(x)$ is now known numerically. The result is shown in Fig. 3b.

If we put all the right units back into the result for the $n_y(y)$ distribution, we can estimate what gate voltage can start the formation of the depletion region on the y axis. This happens when the distribution at $y = 0$ becomes equal to the background density n_{0y} . The condition is

$$\frac{eV_{g_c}}{E_F} = -\frac{1}{n_y(y=0)}. \quad (12)$$

In this case, V_{g_c} comes out to be 230 mV.

This result is not in very good agreement with the experimental result⁷. We give two reasons to explain this discrepancy. First, our critical voltage value represents the onset of depletion, which is not exactly when the source-drain channel is cut off. Electrons can still tunnel through if the depletion width is on the order of the Fermi wavelength. Another, less important reason, is the behavior of the 2DEG density close to the boundary. The wave function for the 2DEG can be represented by $\psi(x, z) = \frac{1}{\sqrt{L_z}} e^{k_z z} \sqrt{\frac{2}{L_x}} \sin k_x x$, where L_x and L_z are chosen boundaries for the gas. Under this assumption, we can calculate the density of the gas to be

$$\frac{n_x(x)}{n_{0x}} = 1 - \frac{J_1(2k_F x)}{k_F x}. \quad (13)$$

The effect of this form of charge distribution is to give an effective gate length, which is slightly larger than the geometrical one. To get an estimate for the difference, we calculate the mean of the extra charge distribution which turns out to be

$$\int_0^\infty du u \frac{J_1(2u)}{u} = \frac{1}{2}, \quad u = k_F x.$$

This is an addition of about 30 Å or 0.31 a_0 to the geometrical gate length. We return to this again in Sec. IV.

III. DEPENDENCE OF THE DEPLETION ON THE BIAS VOLTAGE

The Fourier method used in the previous section can not be used when a depletion region is present. The Thomas-Fermi equations do not hold in that case. A numerical solution had to be employed by discretizing $n_x(x)$ and $n_y(y)$, converting the integral equations into matrix equations, and simultaneously solving for the charge distribution everywhere.

Similar to the treatment employed in Sec. II, we first try to investigate the behavior of the distribution for large x and y . We assume that $n_x(x) \sim \frac{\alpha}{x}$ and that $n_y(y) \sim \frac{\beta}{|y|}$ in this limit. First, by considering charge neutrality from Eq. (6), we must have $\int_a^l dx \frac{\alpha}{x} + \int_{-l}^l dy \frac{\beta}{|y|} = 0$, which implies (as $l \rightarrow \infty$) that $\beta = -\frac{\alpha}{2}$. Similarly to Sec. II, we obtain from the limit $\delta_x = \frac{3\pi\alpha}{4}$ and $\delta_y = -\frac{\pi\alpha}{4}$, which combined with the requirement of Eq. (7) gives

$$\delta_x = \frac{3}{4}, \quad \delta_y = -\frac{1}{4} \quad (14)$$

and

$$n_x(x) = \frac{1}{\pi x}, \quad x \rightarrow \infty; \quad n_y(y) = -\frac{1}{2\pi|y|}, \quad |y| \rightarrow \infty. \quad (15)$$

The same results were obtained in Sec. II.

To accommodate depletion, only small changes need to be made to Eqs. (5) and Eq. (6). Assuming a depletion region from $-d/2$ to $d/2$, the new equations are

$$\begin{aligned}
n_x(x) = & \delta_x + \frac{2}{\pi} \int_a^\infty dx' n_x(x') \log|x - x'| \\
& + \frac{4}{\pi} \int_0^{d/2} dy' n_y(y = d/2) \log|x^2 + y'^2|^{1/2} \\
& + \frac{4}{\pi} \int_{d/2}^\infty dy' n_y(y') \log|x^2 + y'^2|^{1/2}
\end{aligned} \tag{16a}$$

and

$$\begin{aligned}
n_y(y) = & \delta_y + \frac{2}{\pi} \int_a^\infty dx' n_x(x') \log|x'^2 + y^2|^{1/2} \\
& + \frac{4}{\pi} \int_0^{d/2} dy' n_y(y = d/2) \log|y^2 - y'^2|^{1/2} \\
& + \frac{4}{\pi} \int_{d/2}^\infty dy' n_y(y') \log|y^2 - y'^2|^{1/2}.
\end{aligned} \tag{16b}$$

Eqs. (16) proved to be a real challenge to solve numerically. The natural logarithms go to $\pm\infty$ when either x or y approaches $\pm\infty$ or 0. Infinities are also encountered whenever $x = x'$ or $y = y'$. To solve these equations the following technique was employed: A cut-off l was introduced on all the integrals. The integrals now have two main parts. One from 0 to l (or $-l$ to l) and another from l to ∞ (or this and $-\infty$ to $-l$). It turns out that we were able to obtain an analytical result to the second portion of these integrals assuming that for large enough l , the $n_x(x)$ and $n_y(y)$ distributions approach their long range approximations. The latter parts of these integrals become tails that we attach to the integrals. The attached tails are

$$\begin{aligned}
t_x(x) = & \frac{2}{\pi} \int_l^\infty dx' \left(\frac{1}{\pi x'} \right) \log|x - x'| \\
& + \frac{4}{\pi} \int_l^\infty dy' \left(\frac{-1}{2\pi|y'|} \right) \log|x^2 + y'^2|^{1/2} \\
& = \frac{2}{\pi^2} \int_0^{x/l} dt \frac{1}{t} \log \left| \frac{(1-t)^2}{1+t^2} \right|^{1/2}
\end{aligned} \tag{17a}$$

with the latter result achieved by setting $t = x/x'$ in the dx' integral, and $t = x/y'$ in the dy' integral. Similarly, we obtain

$$\begin{aligned}
t_y(y) = & \frac{2}{\pi} \int_l^\infty dx' \left(\frac{1}{\pi x'} \right) \log|x'^2 + y^2|^{1/2} \\
& + \frac{4}{\pi} \int_l^\infty dy' \left(\frac{-1}{2\pi|y'|} \right) \log|y^2 - y'^2|^{1/2}
\end{aligned}$$

$$= \frac{2}{\pi^2} \int_0^{y/l} dt \frac{1}{t} \log \left| \frac{1+t^2}{1-t^2} \right|^{1/2}. \quad (17b)$$

With the addition of these tails and the l cut-offs, Eqs. (16) become

$$\begin{aligned} n_x(x) = & \delta_x + \frac{2}{\pi} \int_a^l dx' n_x(x') \log |x - x'| \\ & + \frac{4}{\pi} \int_0^{d/2} dy' n_y(y = d/2) \log |x^2 + y'^2|^{1/2} \\ & + \frac{4}{\pi} \int_{d/2}^l dy' n_y(y') \log |x^2 + y'^2|^{1/2} \\ & + \frac{2}{\pi^2} \int_0^{x/l} dt \frac{1}{t} \log \left| \frac{(1-t)^2}{1+t^2} \right|^{1/2} \end{aligned} \quad (18a)$$

and

$$\begin{aligned} n_y(y) = & \delta_y + \frac{2}{\pi} \int_a^l dx' n_x(x') \log |x'^2 + y^2|^{1/2} \\ & + \frac{4}{\pi} \int_0^{d/2} dy' n_y(y = d/2) \log |y^2 - y'^2|^{1/2} \\ & + \frac{4}{\pi} \int_{d/2}^l dy' n_y(y') \log |y^2 - y'^2|^{1/2} \\ & + \frac{2}{\pi^2} \int_0^{y/l} dt \frac{1}{t} \log \left| \frac{1+t^2}{1-t^2} \right|^{1/2}. \end{aligned} \quad (18b)$$

The neutrality equation (Eq. (6)) also changes to

$$\begin{aligned} & \int_a^l dx n_x(x) + 2 \int_0^{d/2} dy n_y(y = d/2) \\ & + 2 \int_{d/2}^l dy n_y(y) = 0. \end{aligned} \quad (19)$$

Eqs. (18) can now be solved with the additional requirement of Eq. (7). A matrix solution is obtained by discretizing $n_x(x)$ and $n_y(y)$ and solving for those values together with δ_x and δ_y . The solutions for $n_x(x)$ and $n_y(y)$ are shown in Fig. 3. The corresponding solutions for Eq. (7) are $\delta_x = 0.749$ and $\delta_y = 0.251$, which are in very good agreement with the predictions of Eqs. (14).

IV. ADDING WIDTH TO THE ELECTRON GASES

To get a more realistic result from our simple model, we now try to add width to the 2DEGs. Assuming that the 2DEGs are in the ground state and extending from $-g/2$ to

$g/2$, the wave function for either one is then given by $\psi(x) = \sqrt{\frac{2}{g}} \cos(\frac{\pi x}{g})$. To make the numerical calculations easier, we assume a square distribution and pick the width f so that $\int_{-f/2}^{f/2} dx x^2 \frac{1}{b} = \int_{-g/2}^{g/2} dx x^2 \frac{2}{g} \cos^2(\frac{\pi x}{g})$, which gives $f = \sqrt{1 - \frac{6}{\pi^2}} g$. The two quantum wells for the 2DEGs are 200 Å on the x axis and 150 Å on the y axis, which give $b = 1.268 a_0$ and $c = 0.951 a_0$ for the x and y axis square width respectively. The new setup is shown in Fig. 2.

With the addition of width, Eqs. (18) become:

$$\begin{aligned} n_x(x) = & \delta_x + \frac{2}{\pi} \int_a^l dx' n_x(x') \frac{1}{b} \int_{-b/2}^{b/2} dy' \log |(x - x')^2 + y'^2|^{1/2} \\ & + \frac{4}{\pi} \int_0^{d/2} dy' n_y(y = d/2) \frac{1}{c} \int_{-c/2}^{c/2} dx' \log |(x - x')^2 + y'^2|^{1/2} \\ & + \frac{4}{\pi} \int_{d/2}^l dy' n_y(y') \frac{1}{c} \int_{-c/2}^{c/2} dx' \log |(x - x')^2 + y'^2|^{1/2} \\ & + \frac{2}{\pi^2} \int_0^{x/l} dt \frac{1}{t} \log \left| \frac{(1-t)^2}{1+t^2} \right|^{1/2} \end{aligned} \quad (20a)$$

and

$$\begin{aligned} n_y(y) = & \delta_y + \frac{2}{\pi} \int_a^l dx' n_x(x') \frac{1}{b} \int_{-b/2}^{b/2} dy' \log |x'^2 + (y - y')^2|^{1/2} \\ & + \frac{4}{\pi} \int_0^{d/2} dy' n_y(y = d/2) \frac{1}{c} \int_{-c/2}^{c/2} dx' \log |x'^2 + x'(y^2 + y'^2)^{1/2} + (y^2 - y'^2)|^{1/2} \\ & + \frac{4}{\pi} \int_{d/2}^l dy' n_y(y') \frac{1}{c} \int_{-c/2}^{c/2} dx' \log |x'^2 + x'(y^2 + y'^2)^{1/2} + (y^2 - y'^2)|^{1/2} \\ & + \frac{2}{\pi^2} \int_0^{y/l} dt \frac{1}{t} \log \left| \frac{1+t^2}{1-t^2} \right|^{1/2}. \end{aligned} \quad (20b)$$

The above equations can be solved in a manner similar to that used in solving Eqs. (18). The results are shown in Fig. 3. Fig. 4 shows a plot of the depletion width vs. applied voltage for different values of the gate length. Fig. 5 shows a plot of the applied voltage needed to create a given depletion width vs. the gate length for various depletion widths.

We now try to again compare these results with the experimental ones. The experimental critical voltage is 450 mV which corresponds to $\frac{eV_c}{E_{Fy}} \approx 50$, shown on Fig. 5. Assuming an effective gate length of about $3 a_0$, this corresponds to a depletion length of approximately $4.5 \lambda_{Fy}$. Fig. 6 shows the voltage distribution on the y axis for various depletion widths.

V. AN APPROXIMATE ANALYTIC APPROACH

Following work done by D. B. Chklovskii et al.⁹, we make the assumption that the potential is constant across the 2DEGs, just like it is in metals. From now on, we will refer to this as the metal approximation. The depletion region can be modeled by a continuous positive charge distribution. This is shown in Fig. 7, along with all the different boundary conditions. To obtain the potential everywhere, we use conformal mapping to transform to a region where potential calculations will be easier. In this section, we switch the labels for the x and y axis to make the conformal mapping transformation easier. The transformation to do this is

$$w = \sin^{-1}(z/l); \quad z = x + iy, \quad w = u + iv. \quad (21)$$

Under this transformation, $-l$ and l go to $-\pi/2$ and $\pi/2$ respectively, and a goes to $a' = \sinh^{-1}(a/l)$. The boundary condition along the depletion region now becomes

$$-\frac{\partial \Phi}{\partial v} \bigg|_{v=0^+} + \frac{\partial \Phi}{\partial v} \bigg|_{v=0^-} = \frac{en_0}{\epsilon} l \cos u. \quad (22)$$

We examine the simpler case, where $a = 0$, which implies that a' in the transformed coordinates is now also zero. From symmetry, we need only to consider the region $0 \leq u \leq \pi/2$. The potential is

$$\Phi_+(u, v) = -V_g + \frac{2V_g}{\pi} u + \sum_{m=\text{even}} A_m \sin(mu) e^{-mv} \quad (23)$$

and

$$\Phi_-(u, v) = \sum_{k=\text{odd}} B_k \cos(ku) e^{kv} \quad (24)$$

above and below the u axis respectively.

By applying the boundary condition of Eq. (22) and the fact that the two potentials have to match at the boundary, we can get equations for the A and B coefficients. The equation for the B coefficients is

$$\begin{aligned} \sum_{k=\text{odd}} \frac{1}{m-k} \left(\frac{eB_k}{E_F} \right) &= \frac{2}{m^2-1} \left(\frac{d}{a_0} \right) \\ &\quad - \frac{1}{m} \left(\frac{eV_g}{E_F} \right); \quad m = \text{even}. \end{aligned} \quad (25)$$

It turns out that the electric field, in the x direction along the boundary, has a singularity when $x = l$ (Ref. 9). This can be canceled by the right choice of l , which is what determines the relation between the applied voltage and the depletion length. In the uv coordinates, the electric field E_x , along the x axis, transforms to

$$-\frac{\partial \Phi}{\partial x} \Big|_{y=0, x \rightarrow l} = -\lim_{u \rightarrow \pi/2} \frac{1}{l \cos u} \frac{\partial \Phi}{\partial u} \Big|_{v=0, u \rightarrow \pi/2}. \quad (26)$$

To cancel the $1/l \cos u = 1/\sqrt{l^2 - x^2}$ singularity, we must have $-\frac{\partial \Phi}{\partial v} \Big|_{v=0, u \rightarrow \pi/2} = 0$, which gives the condition

$$\sum_{k=\text{odd}} (-1)^{(k+1)/2} k \left(\frac{eB_k}{E_F} \right) = 0. \quad (27)$$

A numerical solution is employed to solve for the depletion region width vs. applied voltage. The result is

$$\frac{d}{a_0} = \frac{2}{\pi} \frac{eV_g}{E_F}. \quad (28)$$

The above equation predicts a linear relationship between the applied voltage and depletion length. It also predicts that $V_{gc} = 0$. This is shown in Fig. 4. The $2/\pi$ slope is in exact agreement with the numerical results.

Finally, we try to investigate another configuration by using the metal approximation.

We assume that the transistor has another gate on the other side, so that the new configuration is now in the shape of a “cross”. This adds more symmetry to the problem, which actually makes the solution under the metal approximation easier. We now only have to consider the upper half of the uv plane. The new solution for $a = a' = 0$ is

$$\frac{d}{a_0} = \frac{eV_g}{E_F}. \quad (29)$$

This gives a $\pi/2$ improvement on the slope of the graph of depletion versus voltage over the “T” configuration. We also calculate d vs. V_g for $a \neq 0$. These results are shown in Fig. 8.

The results are in very good agreement with the high bias limit and predict the correct slope between the applied voltage and the depletion width. It should be noted that all the slopes converge to the same value in the limit of high bias voltage. Of course, the “cross” transistor is not a device that can be manufactured with current technology. However, the study of this interesting configuration showed how much improvement an additional mirror gate can give.

VI. CONCLUSION

The Thomas-Fermi equation allows us to get a good sense of the general behavior of depletion formation on the “T” transistor. Because of its simplicity, the metal approximation used in Sec. V provided a very powerful method for checking our results. Such approximation can also be used to get a general idea of a problem without having to explore complicated analytical or numerical solutions. And though the method does not predict the correct minimum voltage needed to start the formation of the depletion region, it does give the correct slope and shows good agreement for large bias voltage.

ACKNOWLEDGMENTS

We would like to thank Xiangming Liu for his help and guidance with some of the numerical problems in this paper and L. I. Glazman for his useful discussions on the metal approximation. Also for their useful discussions, G. A. G. would like to thank M. C. Chang, Ertugrul Demircan, and R. Jahnke. This work was supported by the Welch Foundation.

REFERENCES

- ¹ *Nanostructures Physics and Fabrication*, edited by M. A. Reed and W. P. Kirk (Academic, New York, 1989)
- ² T. Ando, A. B. Fowler, and F. Stern *Rev. Mod. Phys.* **54**, 437 (1982).
- ³ A. D. Wieck and K. Ploog, *Appl. Phys. Lett.* **56**, 928 (1990).
- ⁴ H. Pothier, J. Weis, R. J. Haug, K. v. Klitzing, and K. Ploog, *Appl. Phys. Lett.* **62**, 3174 (1993).
- ⁵ M. A. Kastner, *Rev. Mod. Phys.* **64**, 849 (1992).
- ⁶ Masami Ishii, Kazuhiko Matsamuto, Hidehiro Morozumi, Yoshinobu Sugiyama, and Tsuneroni Sakamoto, *Jpn. J. Appl. Phys.* **32**, L36 (1993).
- ⁷ H. L. Stormer, K. W. Baldwin, L. N. Pfeiffer, and K. W. West, *Appl. Phys. Lett.* **59**, 9 (1991).
- ⁸ X. Liu, and Q. Niu, *Phys. Rev. B* **46**, 16 (1992).
- ⁹ D. B. Chklovskii, B. I. Shklovskii and L. I. Glazman *Phys. Rev. B* **46**, 7 (1992).

FIGURES

FIG. 1. Schematic cross section of the T-FET. The two 2DEGs are shown in the gray shaded areas.

FIG. 2. The system of coordinates chosen for the model. We always assume that the positive donors are found where the 2DEGs (shaded areas) are.

FIG. 3. The electron distributions for the gate (x axis) and source-drain (y axis) channels are shown for different depletion lengths d and with or without assumed width for the 2DEGs. Lengths are in units of a_0 , and electron distributions are in units of $\frac{eV_g}{E_F}n_0$.

FIG. 4. Plots of the depletion length d as a function of applied voltage V_g for different gate lengths a . From left to right, the solid lines correspond to gate lengths $\frac{a}{a_0} = 0, 1, \dots, 8$. The dotted line corresponds to the prediction of the metal approximation for $\frac{a}{a_0} = 0$.

FIG. 5. A plot of the applied voltage V_g , required to produce a given depletion width d , as a function of the gate length a . From bottom to top, the solid lines correspond to depletion widths $\frac{d}{a_0} = 0, 5, 10, 15, 20$ ($5 a_0 = 1 \lambda_{Fy}$). The dotted line corresponds to the experimental critical voltage of 450 mV .

FIG. 6. A plot of the potential energy $U_y(y)$, in units of the Fermi energy, along the y axis for a depletion $\frac{d}{a_0} = 5, 10, 15, 20$ ($5 a_0 = 1 \lambda_{Fy}$). The dotted line represents the Fermi level.

FIG. 7. The boundary conditions for the potential in both the xy and uv coordinate systems. The transformation is $w = \sin^{-1}(z/l)$, with $z = x + iy$ and $w = u + iv$. The solid lines are the positive background charge, and the dotted lines are the 2DEGs, which are assumed to be at a constant potential.

FIG. 8. Depletion length d vs. applied voltage V_g for the “cross” transistor using the metal approximation for different gate lengths a . From left to right the solid lines correspond to $\frac{a}{a_0} = 0, 1, \dots, 5$.

AlGaAs

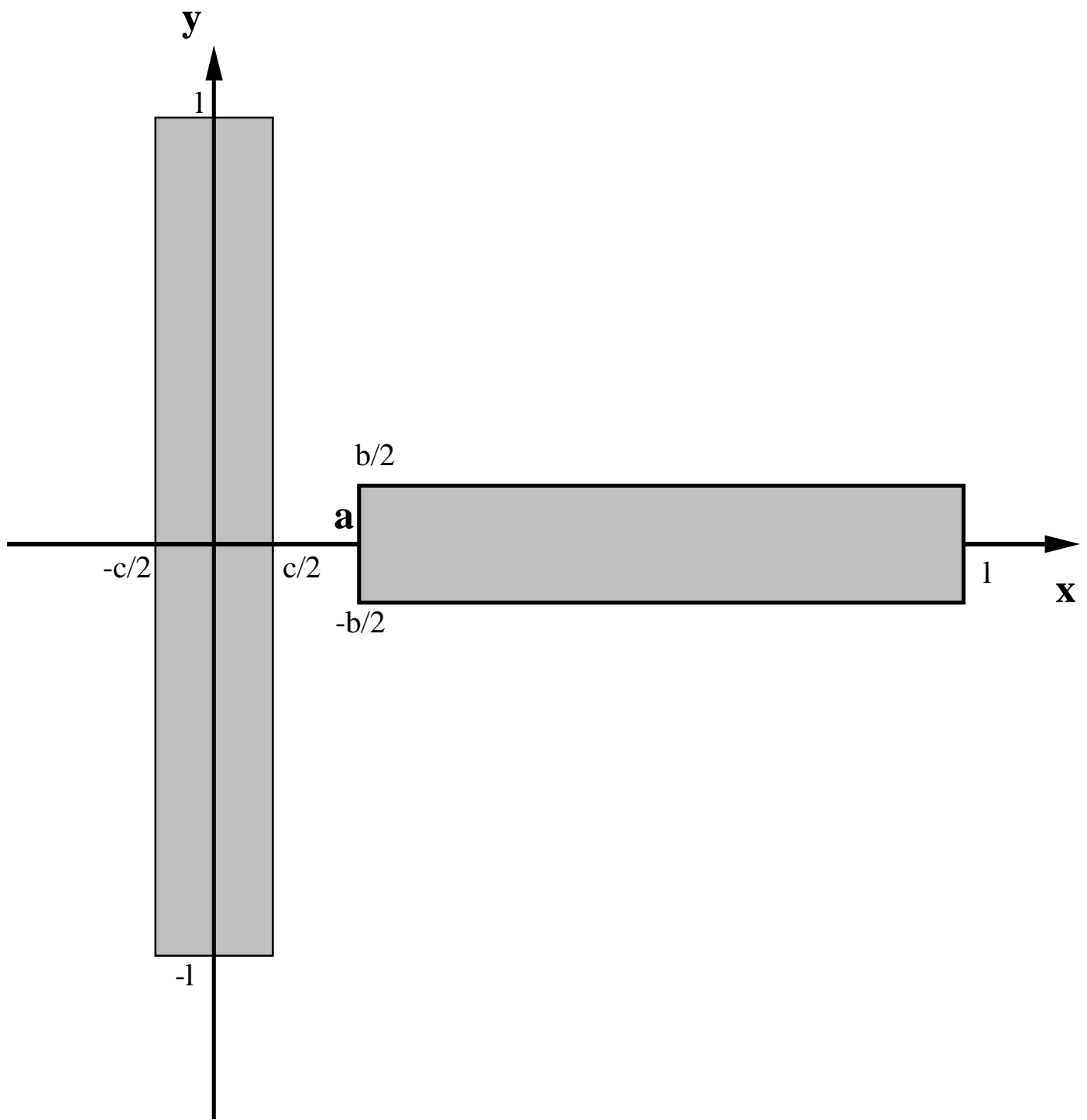


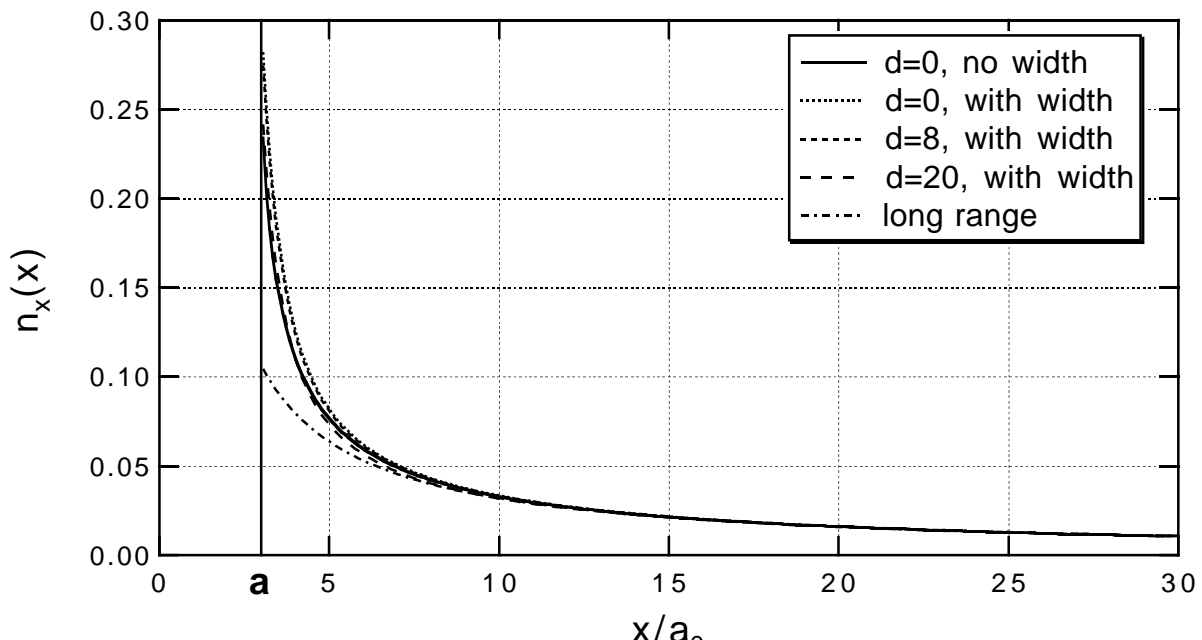
AlGaAs



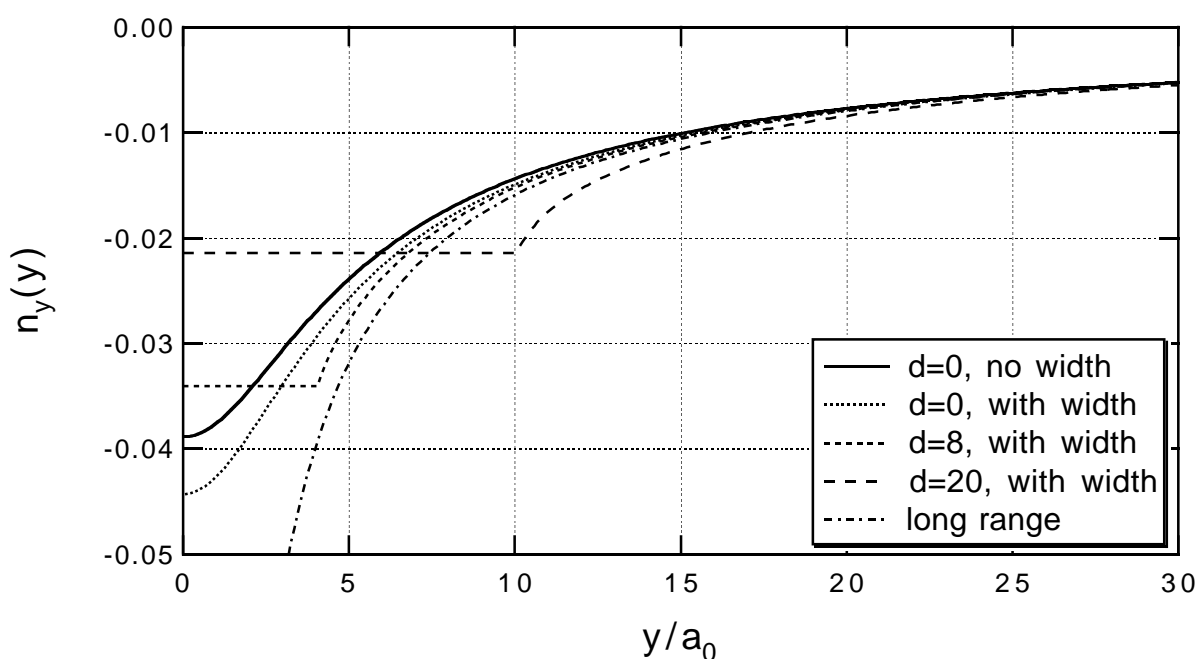
AlGaAs







(a)



(b)

